Microbial inoculation shapes local and systemic grapevine microbiota and wine metabolites across ages and managements.

Beatrice Buffoni[1†], Matteo Chialva[1†], Nicola Cavallini[2], Teresa Mazzarella[1], Elio Padoan[3], Cristina Votta[1], Alex Berriolo[4], Anaïs Poirier[5], Francesco Savorani[2], Sergio Capaldo[6], Luisa Lanfranco[1], Eva López-Rituerto[7], Isabelle Masneuf-Pomarede[5,8], Valentina Fiorilli[1*]

1. Department of Life Sciences and Systems Biology, University of Turin, Viale Mattioli 25, 10125 Turin, Italy.
2. Department of Applied Science and Technology, Polytechnic of Turin, Corso Duca degli Abruzzi 24, 10129 Turin, Italy.
3. Department of Agricultural, Forest and Food Sciences, University of Turin, Largo Paolo Braccini 2, 10095 Grugliasco (TO), Italy
4. PeqAgri Società agricola A.r.l, Strada del Castello-Colla Micheri 20- 17051- Andora (SV)
5. Univ. Bordeaux, Bordeaux INP, INRAE, OENO, UMR 1366, ISVV, 33140 Villenave d'Ornon, France.
6. La Granda S.r.l. Via Garetta 8/A 12040 Genola (CN).
7. Estación Enológica de Haro, Consejería de Agricultura, Ganadería, Mundo Rural y Medio Ambiente, Av. Bretón de los Herreros 4, 26200 Haro, La Rioja, Spain.
8. Bordeaux Sciences Agro, Bordeaux INP, INRAE, OENO, UMR 1366, ISVV, 33170 Gradignan, France.

†Beatrice Buffoni and Matteo Chialva contributed equally to this work.

*Correspondence

Valentina Fiorilli, Viale Mattioli 25, 10125 Turin, valentina.fiorilli@unito.it.

Supplementary Information

Supplementary Figures

Figure S1. Satellite image of the study area with the boundaries of the two vineyards analyzed in this work.

Figure S2. Schematic overview of the experimental setup.

Figure S3. Rarefaction curves of 16S and ITS rDNA libraries of soil, rhizosphere and endosphere samples.

Figure S4. Shannon diversity index values (α-diversity) of grapevine microbial communities.

Figure S5. Differential abundance of prokaryotes and fungi in treated versus control in both vineyards.

Figure S6. Rarefaction curves of 16S and 18S rDNA libraries of grape samples.

Figure S7. Quantification of the leaf ionome profile of *Vitis vinifera* var. Pigato under microbial inoculum and control treatments in the two studied vineyards.

Figure S8. Quantification of the must metabolites of *Vitis vinifera* var. Pigato under microbial inoculum and control treatments in the two studied vineyards.

Figure S9. sPLS-DA model (DIABLO) tuning and diagnostics.

Figure S10. Cross-block associations on higher-order components (2-4) of the DIABLO (multiblock sPLS-DA).

Supplementary Tables

Table S1. Physico-chemical characterization of soils collected from both vineyard sites (VN and VO).

Table S2. PERMANOVA table (adonis, 9999 permutations) of the Bray-Curtis dissimilarities of root-associated prokaryotic and fungal microbial communities.

Table S3. PERMANOVA table (adonis, 9999 permutations) of the Bray-Curtis dissimilarities for grape-associated bacterial and fungal microbial communities.

Table S4. Differentially-abundant taxa of grapes-associated communities (Prokaryotes and Fungi) in treated vs control samples in both VN and VO sites (DESeq2, FDR<0.05).

Supplementary Dataset (as additional files)

Dataset S1. Raw reads count and ASVs calling statistics for 16S and ITS2 rDNA amplicon libraries obtained from root-associated compartments.

Dataset S2. Raw reads count and ASVs calling statistics for 16S and ITS2 rDNA amplicon libraries obtained from grapes.

Supplementary Figures

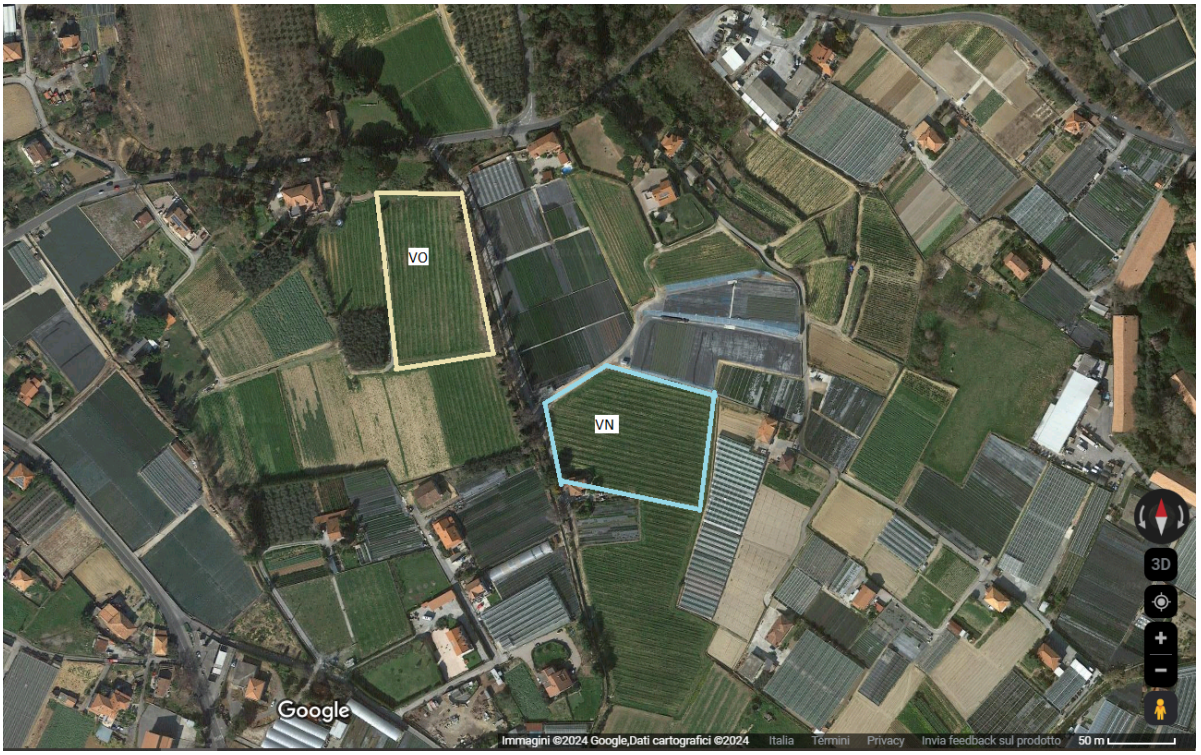

Figure S1. Satellite image of the study area with the boundaries of the two vineyards analyzed in this work. The delineated contours indicate the exact extent of each vineyard (VO, in yellow; VN in light blue) selected for analyses. Google, Map Data @2024.

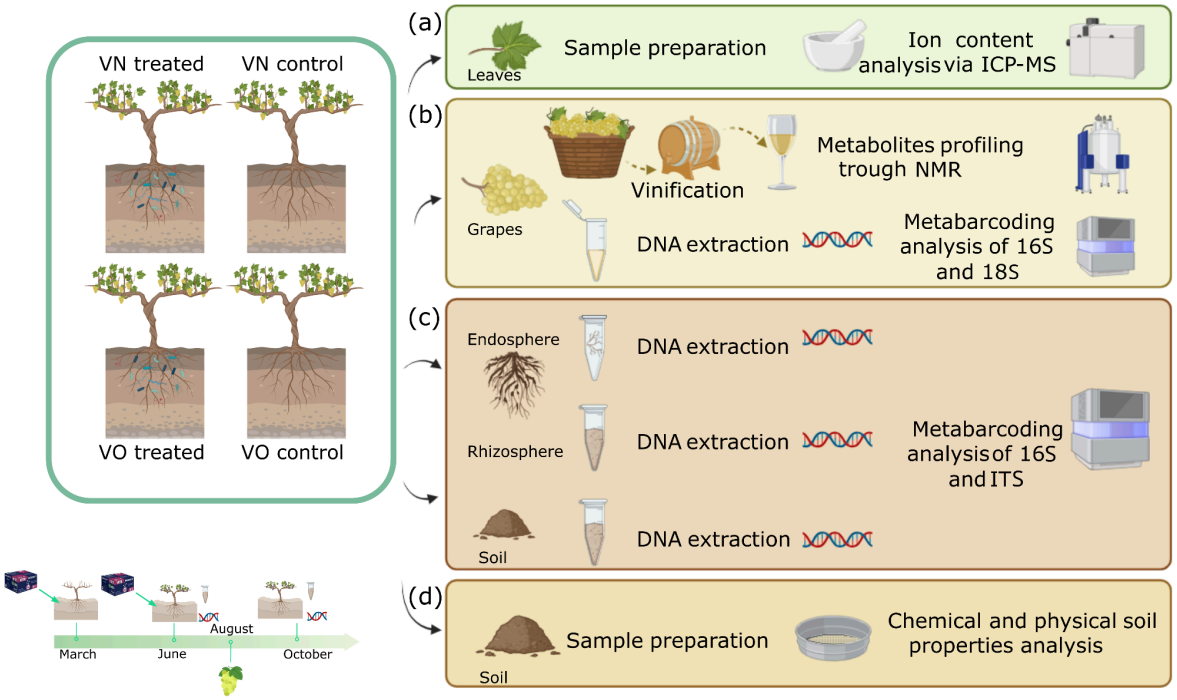

Figure S2. Schematic overview of the experimental setup. In both vineyards (VN and VO), 100 plants were treated with a commercial bioinoculum (Treated) in March and June of 2022 and 2023, while 100 untreated plants served as controls (Control). Root, soil, and rhizosphere samples were collected in June and October, and grape samples in August in both years (2022, 2023). For each condition (VN-Treated, VN-Control, VO-Treated, VO-Control), the following samples were obtained: (**a**) leaves for ionome profiling by ICP-MS; (**b**) grapes for vinification, with grape must and wine analyzed by NMR for metabolite profiling; additional grapes were pressed for DNA extraction and metabarcoding analysis of 16S and 18S; (**c**) roots and soils from five different plants pooled into one biological replicate. The root endosphere was separated from the rhizosphere, and DNA was extracted from root, soil, and rhizosphere for metabarcoding analysis of 16S and ITS; (**d**) soil samples for chemical and physical property analyses.

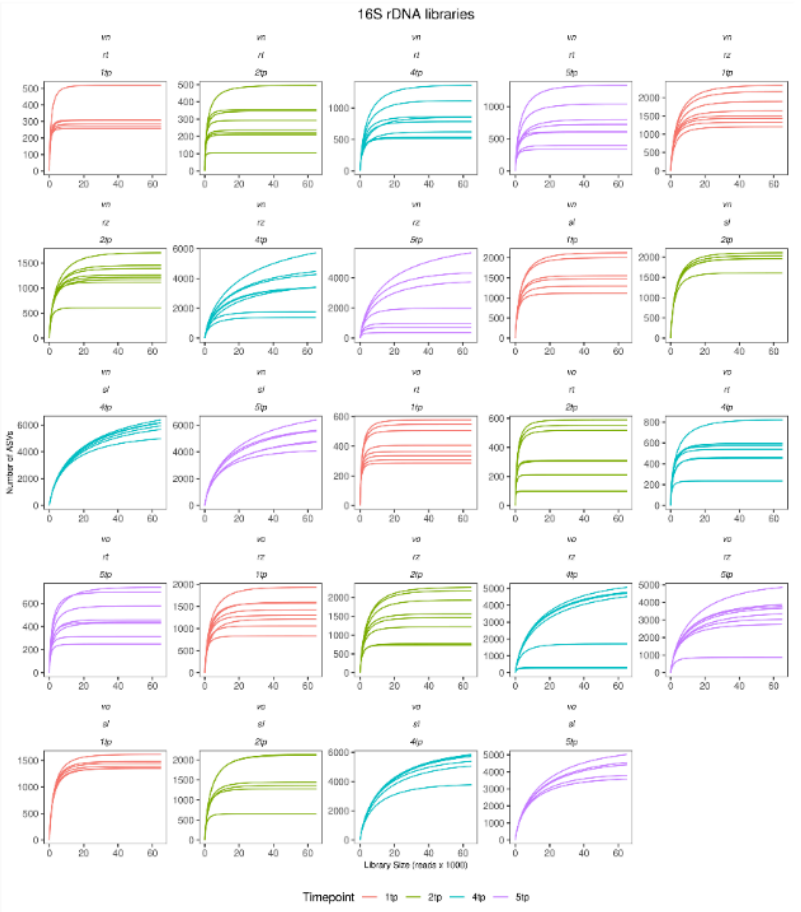

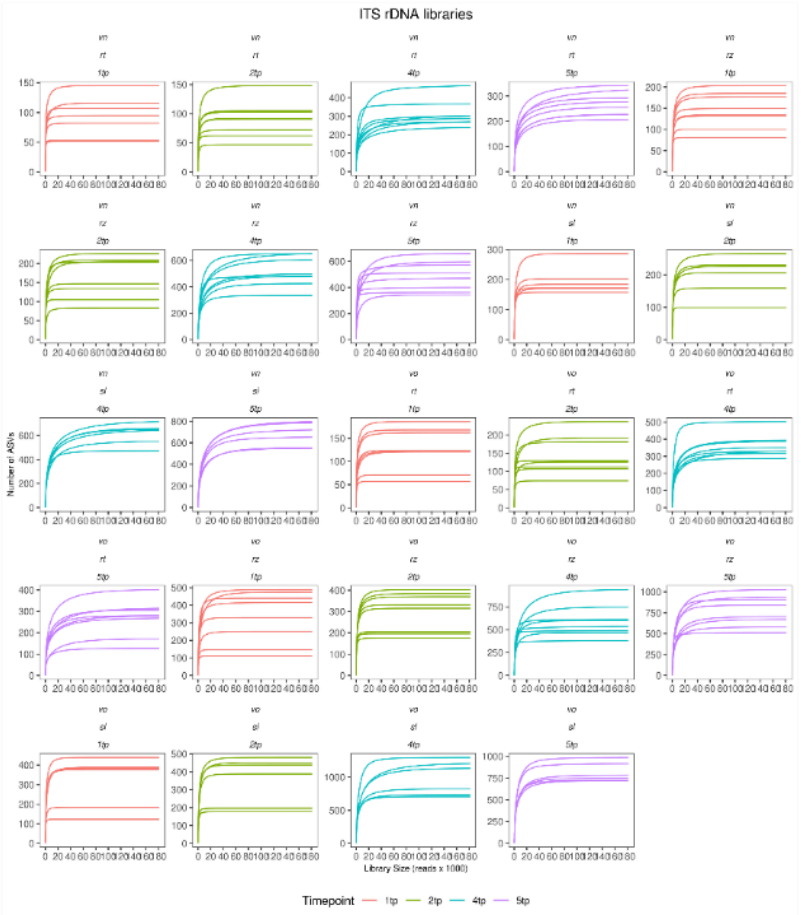

Figure S3. Rarefaction curves of 16S and ITS rDNA libraries of soil, rhizosphere and endosphere samples. Each plot represents the sample per condition (vineyard, compartment and timepoint). Abbreviations: rt - root endosphere, rz - rhizosphere, sl - soil, 1tp and 4tp are referred to the flowering, while 2tp and 5tp are referred to ripening.

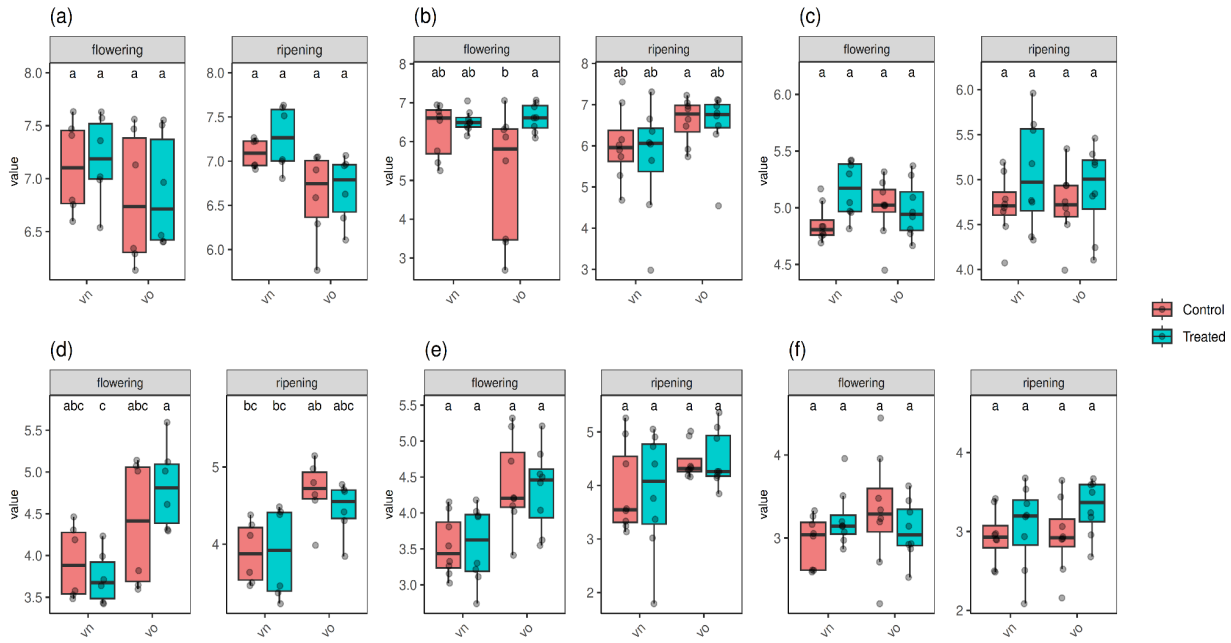

Figure S4. Shannon diversity index values (α-diversity) of grapevine microbial communities. Plots are grouped by site (x-axis), treatment (color) and phenological stage (sub-plots) for prokaryotic (**a**-**c**) and fungal (**d**-**f**) amplicon libraries. Values from different root-associated compartments, including bulk soil (**a**,**d**), rhizosphere (**b**,**e**) and root endosphere (**c**,**f**) are shown in different plots. In each plot points represent values from each single library. Flowering phenological stage, BBCH stage 7 (June 2022-2023, flowering) and ripening phenological stage, BBCH stage 9 (October 2022-2023, ripening) were studied. Boxplots display the median (horizontal line), the quartiles (boxes) and 1.5 × interquartile range (whiskers). Letters indicate significant differences between sites and treatment according to Tukey's post-hoc test after ANOVA ($p < 0.05$).

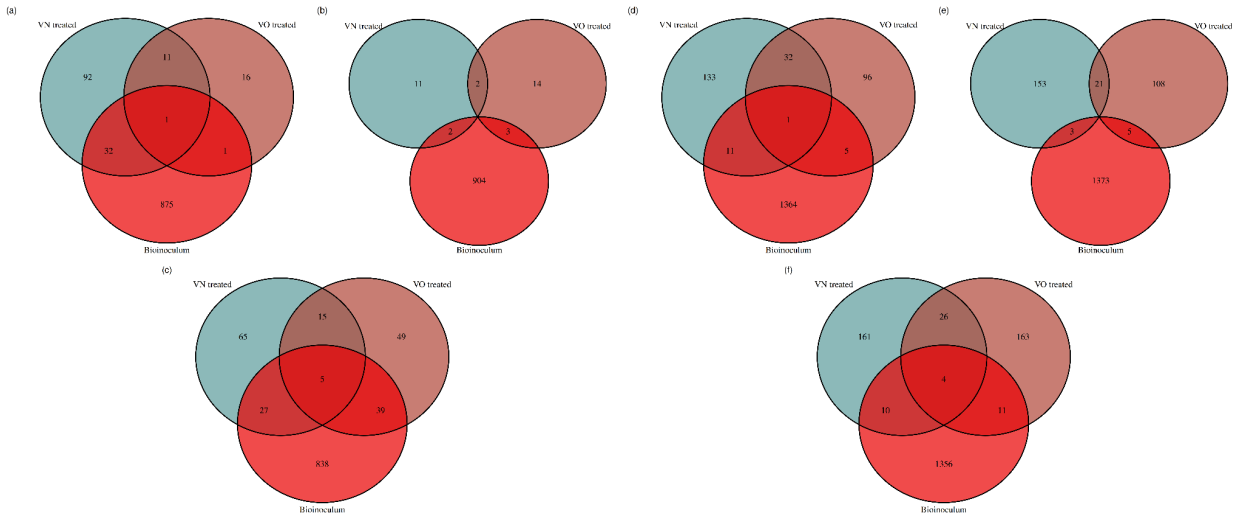

Figure S5. Differential abundance of prokaryotes and fungi in treated *versus* control in both vineyards. (**a-c**) Number of enriched bacterial ASVs in the three compartments considered (a, soil; b, rhizosphere; c, endosphere). (**d-f**) Number of enriched fungal ASVs in the three compartments considered (d, soil; e, rhizosphere; f, endosphere).

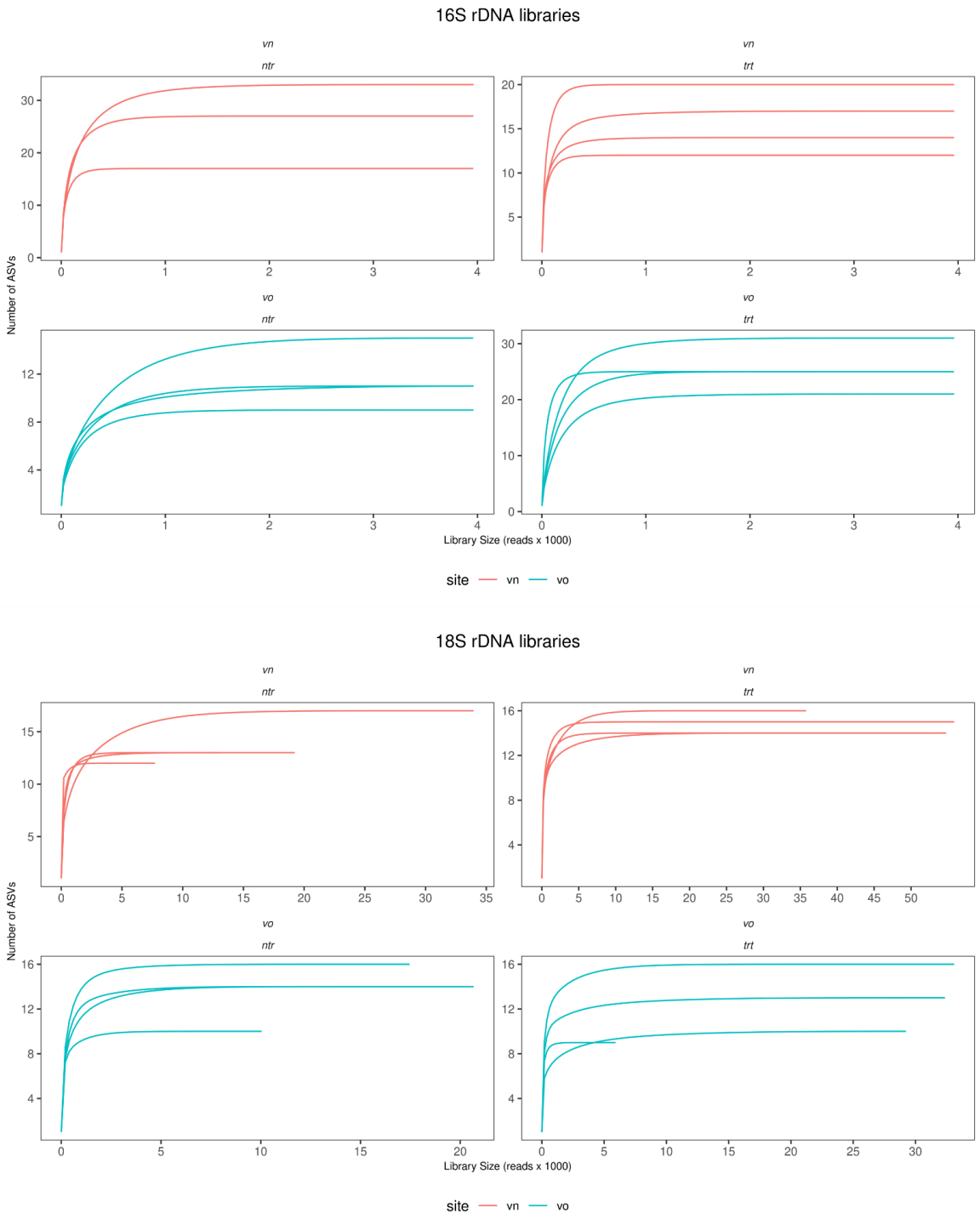

Figure S6. Rarefaction curves of 16S and 18S rDNA libraries of grape samples. Each plot represents the sample per condition (vineyard, treatment). Abbreviations: trt - Treated, ntr - Control.

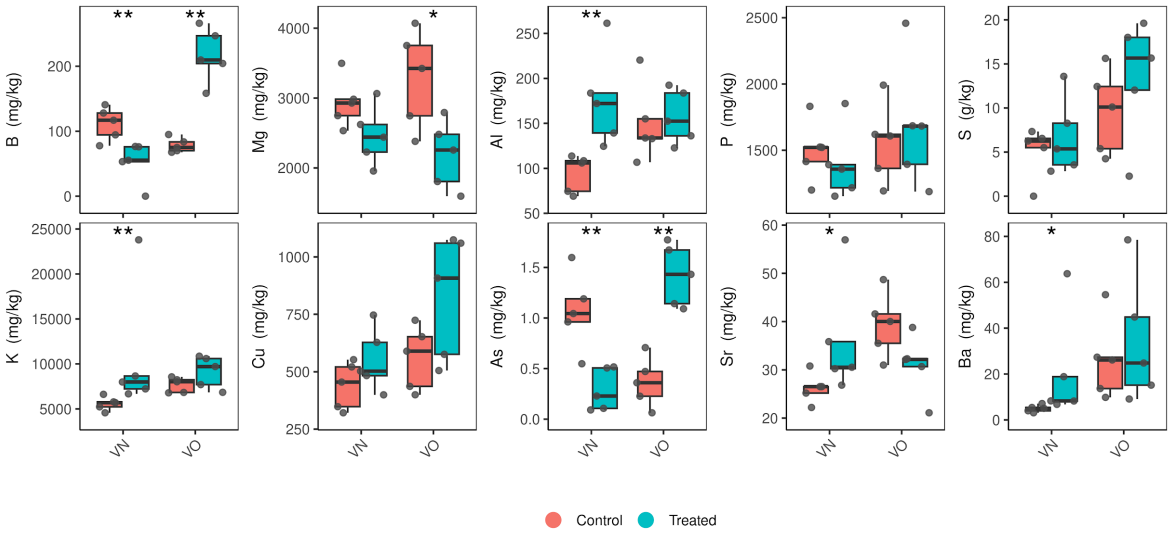

Figure S7. Quantification of the leaf ionome profile of *Vitis vinifera* var. Pigato under microbial inoculum and control treatments in the two studied vineyards. Plots are grouped by site (x-axis) and treatment (color). Values from each ion are shown in different plots. In each plot points represent values from each single sample. Chemical elements are aluminium (Al), arsenic (As), boron (B), barium (Ba), copper (Cu), potassium (K), magnesium (Mg), phosphorous (P), sulphur (S) and strontium (Sr). Boxplots display the median (horizontal line), the quartiles (boxes) and 1.5 × interquartile range (whiskers). Asterisks indicate significant differences between sites and treatment according to Tukey's post hoc test after ANOVA ($p < 0.05$).

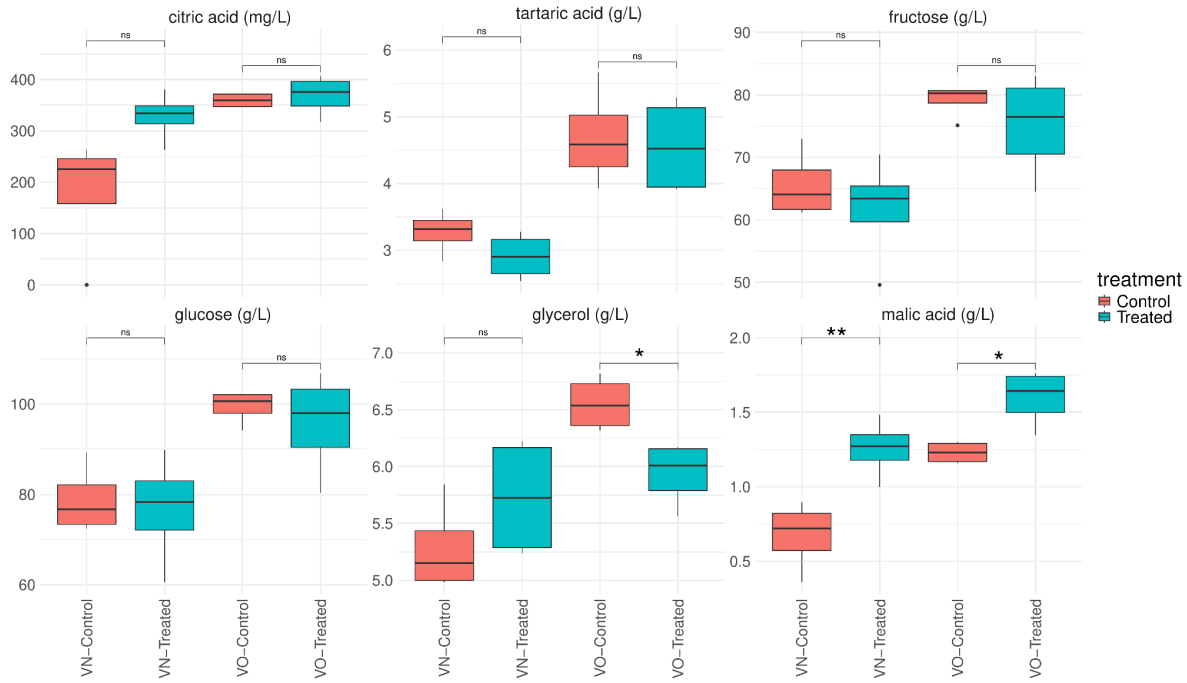

Figure S8. Quantification of the must metabolites of *Vitis vinifera* var. Pigato under microbial inoculum and control treatments in the two studied vineyards. Plots are grouped by condition (site - treatment) (x-axis and color). Values from each metabolite are shown in different plots. Boxplots display the median (horizontal line), the quartiles (boxes) and 1.5 × interquartile range (whiskers). Asterisks indicate significant differences between sites and treatment according to Tukey's post hoc test after ANOVA ($p < 0.05$).

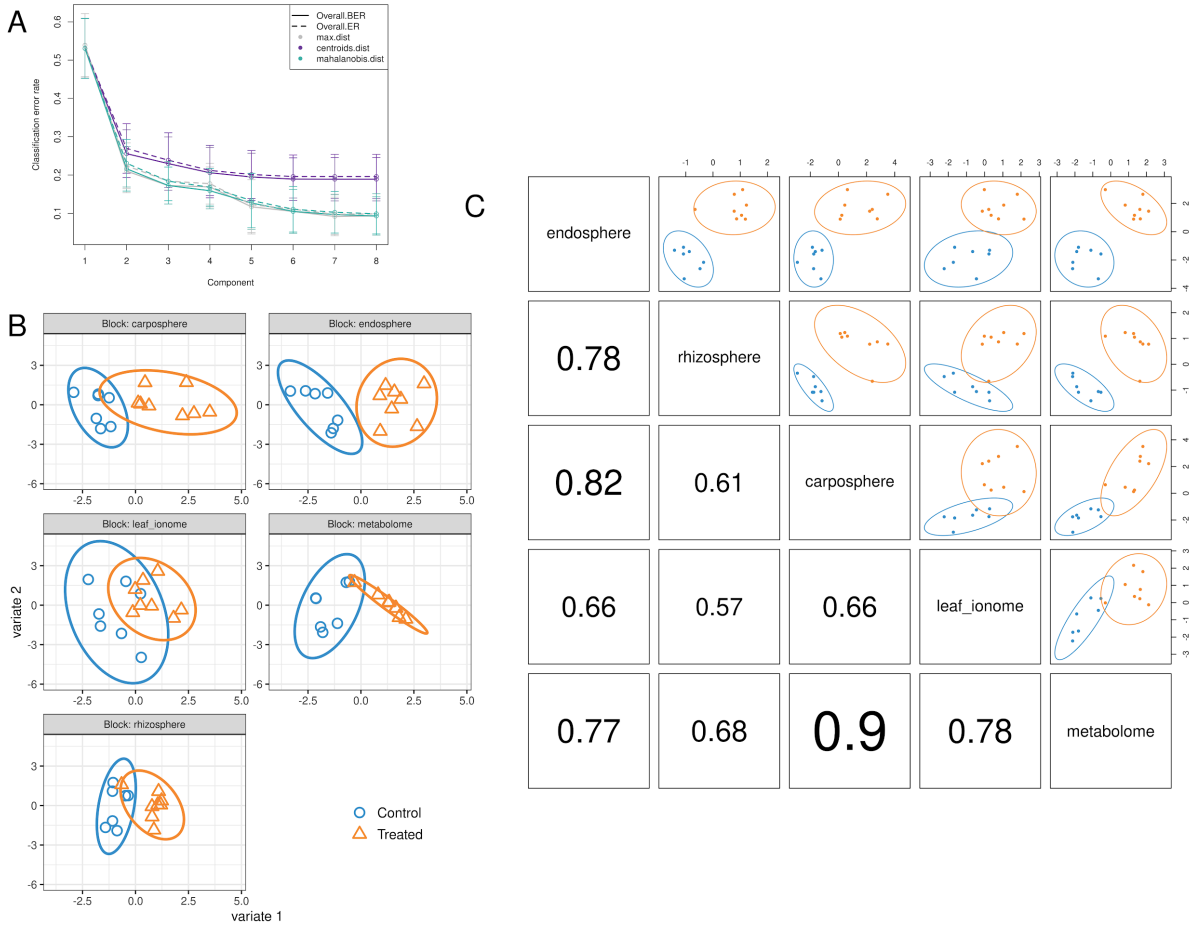

Figure S9. sPLS-DA model (DIABLO) tuning and diagnostics. (**A**) Selection of the optimal number of components; classification error rates (balanced overall) are represented on the y-axis; the number of components is reported on the x-axis for each prediction distance. (**B**) Sample plots for each block based on the first two variates; points in scatter plots represent samples and are coloured by treatment type; 95% confidence ellipses are shown. (**C**) Pairwise correlations of the first variate across all blocks; in the upper panels, points in scatter plots show samples and are coloured by treatment type; 95% confidence ellipse are shown, while the lower panels report the pairwise correlation coefficients between the first variate of each block.

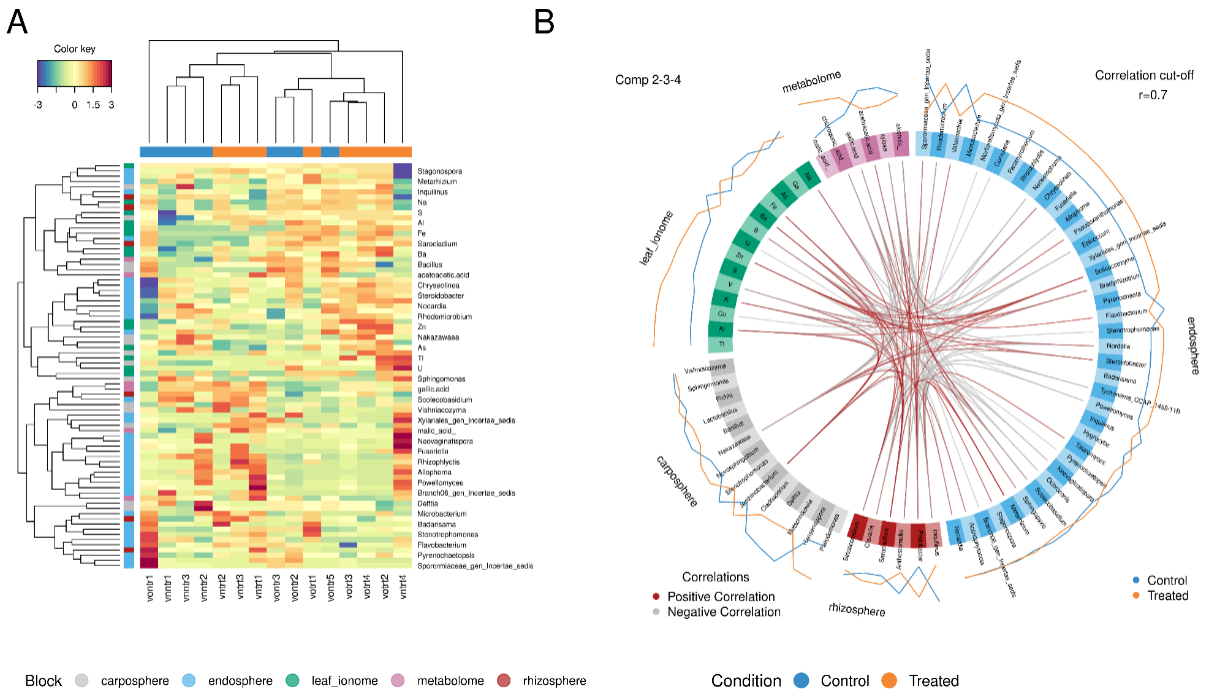

Figure S10. Cross-block associations on higher-order components (2-4) of the DIABLO (multiblock sPLS-DA). (**A**) Clustered image map (CIM) showing sample similarities (columns) and inter-block (rows) variable correlations obtained from the DIABLO model on components 2–4 at > 0.7 correlation threshold. (**B**) Circos plot illustrating direct correlations between variables across different blocks obtained from the DIABLO model on components 2–4; outer tracks indicate average abundance of each variable within each block in Treated and Control samples: only inter-block correlations higher than 0.7 are shown.

Supplementary Tables

Table S1. Physico-chemical characterization of soils collected from both vineyard sites (VN and VO).

Variables	VO	VN	p-value	Signif.
pH	7.30 ± 0.05	7.54 ± 0.01		
Carbonates (%)	1.13 ± 0.13	2.63 ± 0.26	0.00001	***
Total N (%)	0.21 ± 0.02	0.15 ± 0.01	0.00115	**
Organic C (%)	1.99 ± 0.24	1.48 ± 0.13	0.0113	
C/N ratio	13.3	9.9	0.007	**
Available P (mg P kg^{-1})	18.37 ± 1.31	29.8 ± 1.67	0.00000	***
Cation Exchange Capacity (meq/100g)	9.13 ± 1.01	7.47 ± 0.43	0.00474	**
Ca exchangeable (meq/100g)	10.39 ± 0.74	8.48 ± 0.21	0.00371	**
Mg exchangeable (meq/100g)	1.24 ± 0.08	1.02 ± 0.04	0.00731	**
K exchangeable (meq/100g)	0.7 ± 0.04	0.92 ± 0.31	0.31730	
Clay % (< 2 µm)	6.58 ± 1.02	7.58 ± 0.72	0.06380	
Fine Silt % (2-20 µm)	14.94 ± 1.54	14.75 ± 0.6	0.79100	
Coarse Silt % (20-50 µm)	8 ± 0.88	8.58 ± 1.35	0.40800	
Fine Sand % (50-200 µm)	22.99 ± 4.28	20.5 ± 1.18	0.19440	
Coarse Sand % (200-2000 µm)	47.49 ± 3.79	48.59 ± 2.29	0.61580	

Asterisks indicate significant differences between vineyards according to ANOVA with Tukey's pairwise post-hoc test (* $p < 0.05$, ** $p < 0.01$, *** $p < 0.001$). Values were measured on 3 soil subsamples, mean ± standard deviation for each parameter is indicated.

Table S2. PERMANOVA table (adonis, 9999 permutations) of the Bray-Curtis dissimilarities of root-associated prokaryotic and fungal microbial communities.

Source of variation	Df	SumOfSqs	R2	F	p-value	Explained variance (%)	signif
Prokaryotes (16S)							
treatment	1	0.19	0.0038	1.39	0.1684	0.39	
phenological stage	1	0.59	0.0119	4.32	**0.0012**	1.19	**
year	1	2.8	0.0567	20.47	**0.0001**	5.67	***
site	1	5.68	0.115	41.51	**0.0001**	11.51	***
compartment	2	16.96	0.3436	61.98	**0.0001**	34.36	***
Residual	169	23.13	0.4685			46.85	
Total	175	49.37	1			100	
Fungi (ITS2)							
treatment	1	0.56	0.0093	2.37	**0.0031**	0.93	**
phenological stage	1	0.55	0.0092	2.33	**0.0029**	0.92	**
year	1	2.45	0.0406	10.28	**0.0001**	4.06	***
site	1	5.99	0.0994	25.18	**0.0001**	9.94	***
compartment	2	10.46	0.1735	21.97	**0.0001**	17.35	***
Residual	169	40.26	0.6676			66.76	
Total	175	60.3	1			100	

Significant results ($p<0.05$) are highlighted in bold type.

Table S3. PERMANOVA table (adonis, 9999 permutations) of the Bray-Curtis dissimilarities for grape-associated bacterial and fungal microbial communities.

Source of variation	Df	SumOfSqs	R2	F	p-value	Explained variance (%)	signif
Prokaryotes (16S)							
site	1	0.84	0.3617	9.12	0.0033	36.175	**
treatment	1	0.3	0.131	3.3	0.0546	13.102	.
Residual	12	1.11	0.475			47.58	
Total	14	2.33	1			100	
Fungi (ITS2)							
Site	1	0.41	0.1583	2.67	**0.043**	15.83	*
Treatment	1	0.18	0.0723	1.22	0.275	7.22	
Residual	13	2.01	0.7694			79.94	
Total	15	2.61	1			100	

Significant results ($p<0.05$) are highlighted in bold type.

Table S4. Differentially-abundant taxa of grapes-associated communities (Prokaryotes and Fungi) in treated vs control samples in both VN and VO sites (DESeq2, FDR<0.05).

ASVs	baseMean	log_2FC	adjusted p (FDR)	Domain	Taxonomy	Species	Site
ASV30	26.89	24.23	0.00000018	Eukaryota	Ascomycota; Eurotiomycetes; Eurotiales; Aspergillaceae	unclassified	VO
ASV80	7.96	18.45	0.00008192	Bacteria	Firmicutes; Bacilli, Lactobacillales; Lactobacillaceae; *Lactobacillus*	*Lactobacillus agilis*	VO
ASV13	150.07	2.60	0.03416967	Bacteria	Proteobacteria; Gammaproteobacteria; Enterobacterales; Enterobacteriaceae; *Escherichia-Shigella*	*Escherichia-Shigella sp.*	VO
ASV29	52.53	-25.07	0.00000014	Bacteria	Proteobacteria; Gammaproteobacteria; Xanthomonadales; Xanthomonadaceae; *Stenotrophomonas*	*Stenotrophomonas sp.*	VN
ASV80	7.96	-22.46	0.00000202	Bacteria	Firmicutes; Bacilli; Lactobacillales; Lactobacillaceae; *Lactobacillus*	*Lactobacillus agilis*	VN